



CFD Simulation of Nanosulfur Crystallization Incorporating Population Balance Modeling

Fatemeh Golkhou and Mahmood Tajee Hamed Mosavian

Department of Chemical Engineering, Engineering Faculty, Ferdowsi

University of Mashhad, Mashhad, Iran

(Received: April 7, 2012; Accepted in Revised Form: February 4, 2013)

Abstract: A physical vapor condensation process for synthesizing nanosized sulfur powder as a precursor for various industries was simulated by the use of computational fluid dynamic (CFD) modeling. The phase change, swirl flow and heat transfer taking place inside the cyclone are analyzed along with particle formation via gas condensation method. The population balance model is a mathematical framework for the modeling of crystal size distribution (CSD) and the study of gas-phase changes leading to nucleation of the first solid particles. In this paper the Direct Quadrature Method of Moments is used for solving the transport equations of the moments of the size distribution. The temperature, velocity and particle size distribution ranges inside the cyclone were computed. The results show the formation of nanosulfur particles in 1-7 nm range.

Key words: CFD • Population balance • Crystal size distribution • Moments

INTRODUCTION

Owing to their unique electronic, catalytic, optical and magnetic properties, nanoparticles continue to attract the attention of researchers [1]. Furthermore, Physical modeling of particulate processes such as crystallization has been the subject of intense research over the last half century [2-4]. Hulburt, Katz [5] and Randolph [6] recognized that many problems of particulate dynamics, principally crystallization, could not be easily solved by conventional conservation equations and therefore proposed the population balance approach.

Population balance is an appropriate mathematical framework dealing with crystallization systems which involve nucleation, growth, breakage or aggregation of particles. Such mathematical approach follows the number of entities, such as the way that their presence or occurrence may dictate the behavior of the system under consideration [2-4]. This paper considers the crystallization of Sulfur vapor in turbulent Flow in cyclone using numerical simulations. The employed kinetic model has been coupled with the quadrature

Method of Moments (QMOM) in order to compute the evolution of the crystal population. Wan, *et al.* [7] showed that the moments of the population balance are accurately predicted for the crystallization process; when the flow field is turbulent and the mixing is not ideal in laminar flow and as a result the steady state well mixed solutions are not accurately simulated. Therefore, we consider that the related calculations are performed for steady state conditions. The method of moments, although providing a simple manipulation of the PBE, has numerous restrictions. One of the papers in crystallization which used this method is the one of Ma and Braatz [8]. The conservation laws of mass and energy can be found elsewhere in literature [9]. During recent years, the numerous population balance equations (PBEs) for crystal growth [10], fragmentation and aggregation [11] have been solved).

Theory

Basic Fluid-phase Equations in CFD: The commercial CFD code FLUENT uses conservation equations for momentum and mass combined with an energy

conservation equation to describe heat transfer phenomena [12]. To take into account the highly irregular nature of turbulence, the components of the velocity vector are usually decomposed in the summation of a mean value and fluctuations; so applying Fever-averaging (valid for flows with variable density), the continuity, Navier–Stokes and scalar transport equations become [13].

$$\partial \bar{\rho} / \partial t + \partial / \partial x_i (\bar{\rho} \tilde{U}_i) = 0 \quad (1)$$

$$\begin{aligned} & \partial / \partial t (\bar{\rho} \tilde{U}_i) + \partial / \partial x_j (\bar{\rho} \tilde{U}_i \tilde{U}_j) + \partial / \partial x_i (\bar{\rho} \tilde{u}_i \tilde{u}_j) \\ & = -\partial \bar{\rho} / \partial x_i + (v + \nu_i) \partial^2 \bar{\rho} \tilde{U}_i / \partial x_j \partial x_j \end{aligned} \quad (2)$$

$$\begin{aligned} & \partial / \partial t (\bar{\rho} \tilde{\Phi}_r) + \partial / \partial x_i (\bar{\rho} \tilde{\Phi}_r \tilde{U}_i) + \partial / \partial x_i (\bar{\rho} \tilde{w}_r \tilde{u}_i) = \\ & (\Gamma + \Gamma_r) \partial^2 \bar{\rho} \tilde{\Phi}_r / \partial x_j \partial x_j + \tilde{S}(\Phi) \end{aligned} \quad (3)$$

Where $\bar{\rho}$ and \bar{P} are the mean density and pressure, respectively, ν is the kinematics viscosity, ν_i is the turbulent viscosity, \tilde{U}_i is the Fever-averaged value of the i th component of the fluid mean velocity, u_i is the component of the fluctuation of velocity, ϕ_a and Φ_a are the mean and fluctuating concentration of the a th scalar, Γ and Γ_r ($\Gamma_r = V_r/S_c$) are molecular and turbulent diffusivity, respectively, $\tilde{S}(\Phi)$ is the Fever-averaged chemical source term. The third term on the left-hand side of Eq. (2) is called Reynolds stress tensor which is generated by the decomposition and needs to be closed. The Standard [14], RNG [15] and Realizable [16] κ - ϵ Models Theory are relatively simple approaches based on the eddy-viscosity concept. If the Reynolds Stress Model (RSM) is employed, the problem is closed by solving transport equations for the turbulent stresses [17, 18]. A multiphase model is necessarily used for the multiphase modeling of particle nucleation and growth [19]. In this study, the mixture model was used because it is simple and requires less computational work [12].

Population Balance: The conservation law of number or the population balance in size coordinates (with L as a diameter of a particle) can be written in the form of equation 4 [9, 20].

$$\begin{aligned} & \partial n / \partial t + \partial (G_n) / \partial L + n \partial V / \partial t + \\ & D(L) - B(L) + \sum \dot{V}_i n / V = 0 \end{aligned} \quad (4)$$

The number density function is n ; V is the number of particles per unit volume in the crystal size interval dL . G

is the growth rate of a single crystal, $B(L)$ is the birth rate and $D(L)$ is the death rate of a crystal. One alternative approach is the solution of the transport equations of moments, using a quadrature formula for the closure of unknown terms. Nodes and weights of the quadrature approximation can be evaluated from the moment of the distribution by using a very efficient algorithm [21, 22].

$$\partial w_a / \partial t + \partial / \partial x_i (\tilde{U}_i w_a) - \partial / \partial x_i [\Gamma_r \partial w_a / \partial x_i] = a_a \quad (5)$$

$$\partial L_a / \partial t + \partial / \partial x_i (\tilde{U}_i L_a) - \partial / \partial x_i [\Gamma_r \partial L_a / \partial x_i] = b_a \quad (6)$$

The method has been recently formulated in a direct formulation (Direct quadrature Method of Moments or DQMOM), is based on solution of the following equations:

$$\tilde{m}_k(x, t) = \int_0^{+\infty} \tilde{n}(L : x, t) L^k dL \approx \sum_{a=1}^N w_a L_a^k \quad (7)$$

The zeroth moment represents the number of crystals per unit mass of solvent. The first moment is total length of all crystals per unit mass of solvent, the second and third moments are related to the area and the volume of crystals per unit mass of solvent respectively. The length-averaged crystal size is written as [23]:

$$LI,0 = m1/m0 \quad (8)$$

Nucleation and Growth Rate: When 0.1 mole of sulfur vapor at 718 K with 0.9 mole of nitrogen gas are conducted to the first inlet and 2 moles of nitrogen gas at 223 k enter the second inlet of the cyclone, they mix and quickly cool and the sulfur nanocrystals are formed. Despite all studies, a detailed description of nucleation and growth process is still missing, especially for nanocrystals with a specific shape [24]. In this study, we estimate these parameters by simplifying assumptions; for example, the nucleation rate of sulfur is found 0.00025 1/cm²s at melting point of sulfur [25].

The driving force for crystal growth, according to Gibbs rule, is to minimize the total surface free energy of the system which is approximately linearly related to the total surface area. This indicates that in the nanosized particle, the surface free energy in comparison to the total free energy is close to being negligible and it is one of the main reasons why crystallization has been so difficult to understand in the past [26, 27]. Table 1 shows some data which is necessary for calculating the growth rate of sulfur in the crystallization process:

Table 1: Parameters used for calculation of growth rate

Parameter	Value	Ref.
$C_c(Kmol/m^3)$	63.9	IS Calculated
$C^*(Kmol/m^3)$	0.00001	[25]
$C(Kmol/m^3)$	0.000215	[25]
σ	19	[9]
S	20	[25]
k_d m/s	0.0223	IS Calculated

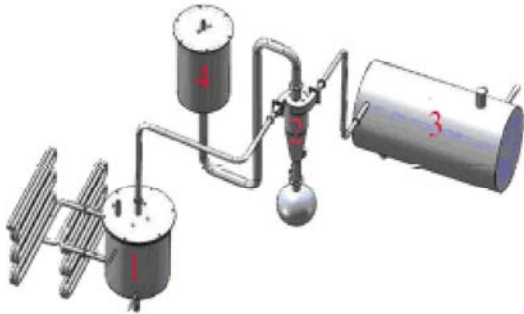


Fig. 1: Nanosulfur synthesis equipment

According to table above, the ratio of C^*/C_c is about 1.6×10^{-7} and it indicates that the heat transfer isn't the effective factor in this case. Also because of $\sigma > 0.5$, the surface combination is negligible [28]. In this case the bulk turbulence is the principal factor controlling the growth rate of particles in the crystallization process. According to Surface Renewal Model of *Danckwerts* the Mass Transfer Coefficient is directly related to the second root of diffusion coefficient. Therefore, the growth rate can be written as relation (9):

Geometry for Simulation : Fig. 1 shows the equipment for synthesis nanosulfur particles via gas condensation method in cyclone:

The solid sulfur which is heated to 718 K with hot nitrogen gas in the 1st vessel enters the cyclone via inlet1 and it mixes quickly with cold nitrogen gas entering via inlet2 (from 3rd vessel). During the crystallization process, the nanosized sulfur particles are created and are carried to up and down outlet of cyclone. We show that most of them are conducting to down outlet of cyclone and some part which remain in the nitrogen flow are trapped in vessel 4 in turbulence water, because of occurring crystallization in the cyclone we only got it for control volume.

The 3D volume grid is represented in Fig. 2. A grid dependence study was conducted to arrive at the appropriate size of the grid for optimal accuracy and efficiency. In the optimal grid, the domain is discretized into a grid of 86732 tetrahedral cells.

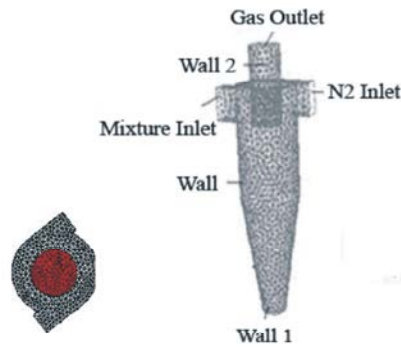


Fig. 2: Three-dimensional tetrahedral grid

The conservation equations for mass, momentum, energy, K-e model and dissipation rate are solved by finite-volume analysis, using a first-order upwind scheme for discretisation of the convective terms in the transport equations. The RNG model is used for modeling of dissipation rate and turbulence kinetic energy.

RESULTS AND DISCUSSION

The results of the simulation are presented below. The solution was converged after more than 42000 iterations. It took more than 12 hours of computation for one run of this 3ddp model on a computer with a dual-core-type 1.67GHz processor and 2GB RAM memory. The range of sulfur particle size in the cyclone is described in Fig. 3.

Results indicate that nanoparticles in the range of 1-6.7 nm are formed in the cyclone via gas condensation method. Also the particle size of the solid phase is related to the mixture temperature. The measured wall temperature profile is shown in Fig. 4.

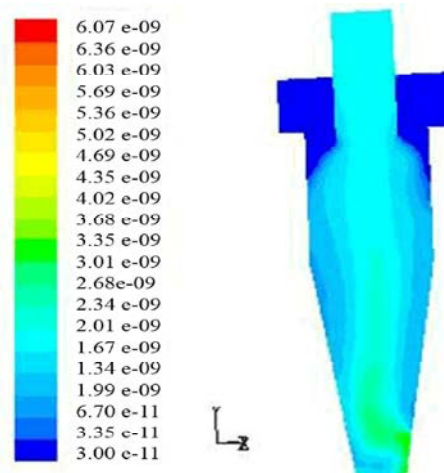


Fig. 3: Range of sulfur particle size along the cyclone (m)

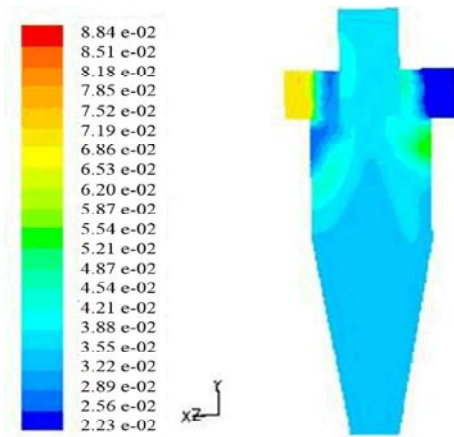


Fig. 4: Contours of total temperature along the cyclone (K)

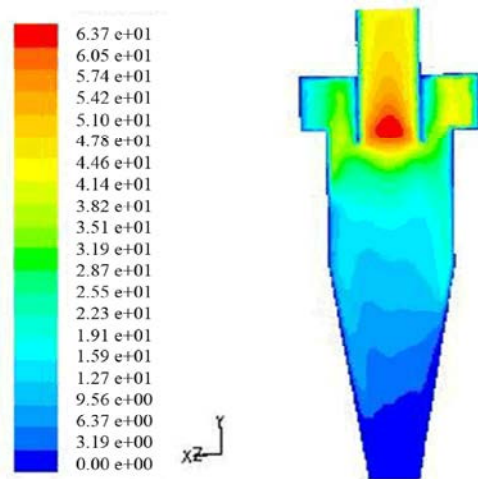


Fig. 5: Velocity magnitudes inside the cyclone (m/s)

As it can be seen in Fig. 4, the temperature in vapor inlet is about 700 k and there is cold nitrogen gas in inlet 2 of the cyclone. After mixing, temperature drops to about 400 k which is the melting point of sulfur and it remains in this temperature. The velocity distribution inside the cyclone is shown in Fig. 6. The color scale indicates the magnitude of the velocity field. The velocity of vapor inlet and nitrogen inlet are 20 and 40 m/s, respectively.

Fig. 5 indicates that the maximum velocity in the cyclone reaches to about 60 m/s around the top outlet of the cyclone and in the lower area it reaches to its minimum level. The size distribution of particles according to the position in the cyclone is shown in Fig. 6. and it reveals that larger particles are produced in lower areas of the cyclone As we can see,

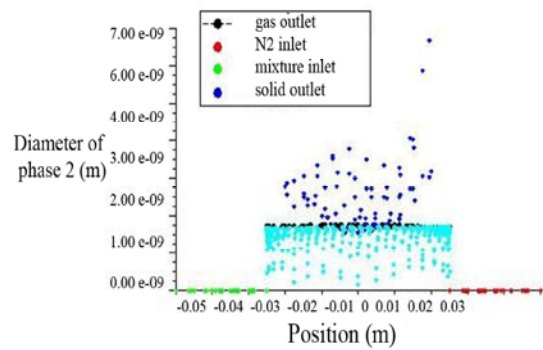


Fig. 6: Size distribution of particles according to position in cyclone

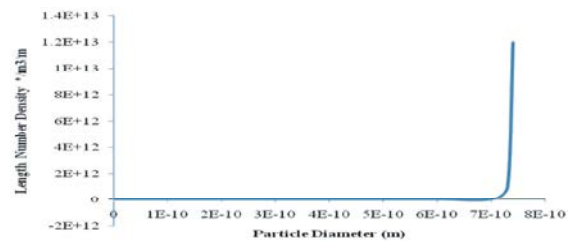


Fig. 7: Number density in terms of particle size

smaller particles under the centrifugal force of the cyclone have been thrown towards the wall. Near the wall, the particle size is large because the velocity is lower there and provides more time for the formation of particles and leads to particle growth. Fig. 8 shows the length number density v.s. particle size of sulfur. The particle number density increases from zero to about 1.2×10^{13} because of changing phase.

The amounts of 0-3rd moments over different surfaces of the cyclone are shown in Fig. 8.

As shown in Fig. 8, the number of crystals in the lower output and the higher inputs of the cyclone reaches zero and accumulation of crystals in the bottom outlet of the cyclone causes it to reach the maximum level of the total length.

TOC Graphic

CFD Simulation of Nanosulfur Crystallization Incorporating Population Balance Modeling: The crystallization process was happened under gas condensation method. Results for velocity, temperature and Particle size distribution are reasonable. The particle size of sulfur computed by software is in the range of 1-7 nm.

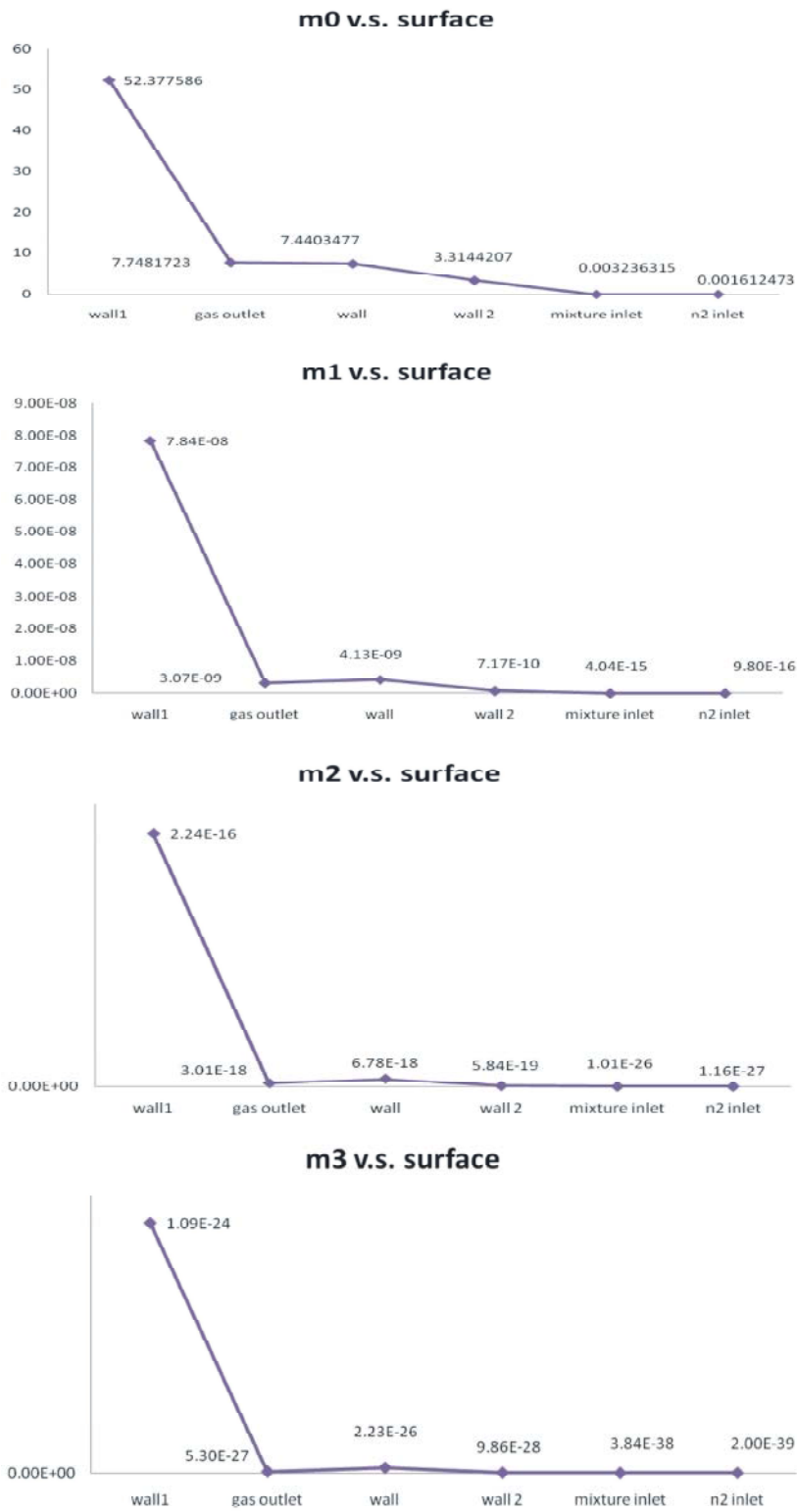


Fig. 8: a) Number of crystals per unit mass of solvent, b) Total length of all crystals per unit mass of solvent, c) Area per unit mass of solvent, d) Volume of crystals per unit mass of solve

CONCLUSIONS

The formation of sulfur nanocrystals were simulated by using the gas condensation technique. A 3D CFD simulation was performed with Fluent to model the crystallization process. After 42000 iterations, results for velocity, temperature profile, particle size distribution (PSD) and density number are reasonable. The final temperature and velocity reach 350 k and 15 m/s respectively. The particle size of sulfur computed by software is in the range of 1-7 nm and it shows that nanocrystals of sulfur can be produced in a cyclone.

Abbreviations

n	=	Number density
V	=	Number of particles per unit volume
dL	=	Crystal size interval
G	=	Growth rate of a single crystal
$B(L)$	=	Birth rate
$D(L)$	=	Death rate of crystal
Φ_a	=	Fluctuating concentration of the a th
Γ	=	Molecular diffusivity
$\Gamma_t = V_t / S_{Ct}$	=	Turbulent diffusivity
$L_a = w_a l_a$	=	a th weighted abscissa'
$C_c (Kmol/m^3)$	=	Molar density of crystal
$C^* (Kmol/m^3)$	=	Solubility
$\bar{\rho}$	=	Mean density
\bar{P}	=	Mean pressure
ν	=	Kinematics viscosity
ν_t	=	Turbulent viscosity
\bar{U}_i	=	Fever-averaged value of the i th
		Component of the fluid mean velocity
u_i	=	Component of the fluctuation of velocity
ϕ_a	=	Mean concentration of the a th scalar
$\bar{S}(\phi)$	=	Favre-averaged chemical source term
σ	=	Relative super saturation
k_d	=	Mass transfer coefficient

REFERENCES

- Gracia-Pinilla, M., E. Martínez, G. Silva Vidaurri and E. Pe'rez-Tijerina, 2010. Deposition of size-selected cu nanoparticles by inert gas condensation. Nanoscale Research Letters, 5(1): 180-188.
- Puel, F., G. Fevotte and J.P. Klein, 2003. Simulation and analysis of industrial crystallization processes through multidimensional population balance equations. part 1: a resolution algorithm based on the method of classes. Chemical Engineering Science, 58(1): 3715-3727.
- Puel, F., G. Fevotte and J.P. Klein, 2003. Simulation and analysis of industrial crystallization processes through multidimensional population balance equations. part 2: a study of batch crystallization. Chemical Engineering Science, 58(1): 3729-3740.
- Ramkrishna, D. and A.W. Mahoney, 2002. Population balance modeling promise for the future. Chemical Engineering Science, 57(1): 595-606.
- Hulburt, H.M. and S. Katz, 1964. Some problems in particle technology. A statistical mechanical formulation. Chemical Engineering Science, 19(1): 555- 574.
- Randolph, A.D., 1964. A population balance for countable entities. Canadian Journal of Chemical Engineering, 42(1): 280-281.
- Wan, B., T.A. Ring, K. Dhanasekharan and J. Sanyal, 2005. Comparison of analytical solutions for scmsmpr crystallizer with qmom population balance modeling in fluent. China Particuology, 3(4): 213-218.
- Ma, D.L. and R.D. Braatz, 2003. Robust identification and control of batch processes. Computer and Chemical Engineering, 27(1): 1175-1184.
- Mersmann, A., 2001. Crystallization Technology Handbook, 2nd Ed. Marcel Dekker: New York.
- Madras, G. and B. McCoy, 2002. Dynamics of crystal size distributions with size-dependent rates. Journal of Crystal Growth, 243(1): 204-213.
- Madras, G. and B.J. McCoy, 2003. . Distribution kinetics of Ostwald ripening at large volume fraction and with coalescence. Journal of Colloid and Interfacial Science, 261(2): 423-433.
- Sohn, H.Y., S. Perez-Fontes and J. Won Choi, 2010. Computational fluid dynamic modeling of a chemical vapor synthesis process for aluminum nanopowder as a hydrogen storage precursor. Journal of Chemical Engineering, 156(1): 215-225.
- Zucca, A., D.L. Marchisio, A.A. Barresi and R.O. Fox, 2006. Implementation of the population balance equation in CFD codes for modeling soot formation in turbulent flames. Chemical Engineering Science, 61(1): 87-95.

14. Yakhot, V. and S.A. Orszag, 1986. Renormalization group analysis of turbulence. I. basic theory. *Journal of Scientific Computing*, 1(1): 1-51.
15. Shih, T., W.W. Liou, A. Shabbir, Z. Yang and J. Zhu, 1995. A new k-epsilon eddy viscosity model for high reynolds number turbulent flows: model development and validation. *Computer and Fluids*, 24(3): 227-238.
16. Launder, B.E. and D.B. Spalding, 1972. *Lectures in mathematical models of turbulence*. Academic: London, England.
17. Launder, B.E., 1989. Second-Moment closure: present . . . and future. *International Journal of Heat and Fluid Flow*, 10(4): 282-300.
18. Launder, B.E., G.J. Reece and W. Rodi, 1975. Progress in the development of a reynolds-stress turbulence closure. *Journal of Fluid Mechanics*, 68(3): 537-566.
19. Fluent, *Fluent 6.3, User's Guide*, Fluent Inc. 2006.
20. Randolph, A.D. and M.A. Larson, 1988. *Theory of particulate processes*. 2nd Ed. Academic: San Diego.
21. McGraw, R., 1997. Description of aerosol dynamics by the quadrature method of moments. *Aerosol Science and Technology*, 27(1): 255-265.
22. Gordon, R.G., 1968. Error bounds in equilibrium statistical mechanics. *Journal of Mathematical Physics*, 9(1): 655.
23. Öncül, A.A., K. Sundmacher, A. Seidel-Morgenstern and D. Thévenina, 2006. Numerical and analytical investigation of barium sulphate crystallization. *Chemical Engineering Science*, 61(1): 652-664.
24. Lim, B., H. Kobayashi, P.H.C. Camargo, L.F. Allard, J. Liu and Y. Xia, 2010. New insights into the growth mechanism and surface structure of palladium nanocrystals. *Nano Research*, 3(1): 180-188.
25. Uchtmann, H., S.Yu. Kazitsyna, F. Hensel, V. Ždímal, B. Tríska and J. Smolik, 2001. Homogeneous and light-induced nucleation of sulfur vapor- diffusion cloud chamber investigations of constant rate supersaturation. *Journal Physical Chemistry B*, 105(1): 11754-11762.
26. Mullin, J.W., 2009. *Crystallization*. 3rd Ed. Oxford
27. Peng, X., 2009. An essay on synthetic chemistry of colloidal nanocrystals. *Nano Research*, 2(1): 425-447.
28. Treybal, R.E., 1980. *Mass transfer operations*. 3th Ed. McGraw-Hill: New York.